B-34 Predicting velocities under stress in anisotropic formations: model and experimental validation

R. PRIOUL[1] and A. BAKULIN[1,2]
[1]Schlumberger Cambridge Research, High Cross, Madingley Road, Cambridge, CB3 0EL, England
[2]Now at Shell Int. E & P, Houston, USA

Summary

Estimating subsurface stress or pore pressure from seismic velocities typically relies on specific petrophysical relationships. Most of the commonly used velocity-stress equations are designed for isotropic media and describe single (P- or S-wave) velocity versus confining stress or depth. Applying such relationships to anisotropic formations under a non-hydrostatic stress state produces significant errors, especially if the relationships were calibrated from log data along deviated wells. Here, we discuss a different way of modelling and calibrating of stress-dependent velocities that uniformly applies to both P- and S-wave velocities and accounts for anisotropy and a non-hydrostatic stress state. We use non-linear elasticity theory that provides straightforward relationships between the full tensor of "effective" elastic stiffnesses and an arbitrary stress state. In the unstressed state, VTI material is described by five elastic stiffnesses. Under stress, analysis of available experimental data on VTI samples suggest that the "effective" stiffness tensor is well described by three "isotropic" non-linear constants. We have applied our physical modelling to two different VTI samples: a strongly anisotropic North Sea shale sample under confining stress and a weakly anisotropic sandstone sample under a biaxial stress cycle. We first demonstrate the success of this simple three-parameter model in predicting V_{P0}, V_{S0} and Thomsen parameters, and second discuss the variation of the anisotropic parameters in both cases. In particular, we observe that, in the case of the weak anisotropic sandstone sample, all the effective anisotropic parameters can be expressed as the sum of the Thomsen coefficient of VTI background and some parameters proportional to the differences in magnitudes of principal stresses, a behaviour which is precisely described by non-linear elasticity under the weak anisotropy approximation. As non-linear coefficients can be derived directly from modern multimode acoustic measurements in the wells, the proposed model represents a powerful tool for predicting stress-dependent anisotropic velocities and for their inversion to stress and pore pressure.

Introduction

The relationship between seismic velocities and effective stress is a critically important element in the seismic characterization and monitoring of the subsurface stress field, either in the overburden or in the reservoir. The growing popularity of multicomponent data means that the S-wave velocity field may be jointly used with the P-wave velocity to accomplish these tasks. Utilizing multicomponent data requires a unified model that links all velocities to stress and accounts for seismic anisotropy. Here, we propose a simple three-parameter model which gives a concise and unified description to anisotropic P- and S- wave velocities under arbitrary stress. The model accounts for the VTI anisotropy of unstressed rocks that may be present in most sedimentary basins.

Theory

"Effective elastic stiffnesses" c_{ij}, defines acoustic velocities under stress, and can be described by the equations of non-linear elasticity for the propagation of small amplitude waves in the presence of initial stresses in the medium (Sinha and Kostek, 1996). When T_{ij} and E_{ij} are corresponding stresses and strains, and one of the principal stresses is vertical ($T_{23} = T_{13} = T_{12} = E_{23} = E_{13} = E_{12} = 0$), the "effective (or stressed) stiffnesses" take a particular simple form following Prioul et al. (2001):

$$
\begin{aligned}
c_{11} &\simeq c^0_{11} + c_{111}E_{11} + c_{112}(E_{22} + E_{33}),\\
c_{22} &\simeq c^0_{11} + c_{111}E_{22} + c_{112}(E_{11} + E_{33}),\\
c_{33} &\simeq c^0_{33} + c_{111}E_{33} + c_{112}(E_{11} + E_{22}),\\
c_{12} &\simeq c^0_{12} + c_{112}(E_{11} + E_{22}) + c_{123}E_{33},\\
c_{13} &\simeq c^0_{13} + c_{112}(E_{11} + E_{33}) + c_{123}E_{22},\\
c_{23} &\simeq c^0_{13} + c_{112}(E_{22} + E_{33}) + c_{123}E_{11},\\
c_{66} &\simeq c^0_{66} + c_{144}E_{33} + c_{155}(E_{11} + E_{22}),\\
c_{55} &\simeq c^0_{44} + c_{144}E_{22} + c_{155}(E_{11} + E_{33}),\\
c_{44} &\simeq c^0_{44} + c_{144}E_{11} + c_{155}(E_{22} + E_{33}),
\end{aligned}
\tag{1}
$$

where $c^0_{11}, c^0_{13}, c^0_{33}, c^0_{44}, c^0_{66}$ ($c^0_{12} = c^0_{11} - c^0_{66}$) represents five stiffnesses for VTI unstressed rock, and c_{111}, c_{112} and c_{123} are third-order (nonlinear) elastic constants describing stress sensitivity ($c_{144} = (c_{112} - c_{123})/2$ and $c_{155} = (c_{111} - c_{112})/4$). Equations (1) have been simplified using the fact that, for rocks, $c_{ijk} \gg c^0_{mn} \gg T_{pq}$. The key assumption in equations (1) is that, although the second-order elastic tensor is described by VTI media, the third-order elastic tensor is approximated by an isotropic form requiring only three third-order constants. Such a description was previously utilized for rocks (Bakulin and Protosenya, 1982); however they used an "isotropic" approximation to convert strain into stress in equations (1). In contrast, we propose to employ VTI Hooke's law exactly. This makes it possible to use confining stress experiments for estimating all three non-linear constants. Clearly, in the general case of triaxial stress ($T_{11} \neq T_{22} \neq T_{33}$), equations (1) describe an orthorhombic medium in which stiffnesses are linearly dependent on principal stresses.

Estimation of non-linear constants for North Sea shale and Colton sandstone

As an example, we tested predictions of non-linear elasticity against experimental lab measurements on two different VTI rocks: a strongly anisotropic North Sea shale sample under confining stress (Hornby, 1995), and a weakly anisotropic Colton sandstone under biaxial stress cycle (Dillen et al., 1999). For the shale sample, the data exhibits a distinctly different behaviour at low and high effective stresses (defined here as the difference between confining and pore pressures), therefore the stress range was divided into two intervals, 5 to 20 and 40 to 100 MPa. For the sandstone sample, one of the directions of the triaxial stress (T_{33}) was aligned with the symmetry axis, and equal compressive stresses ($T_{11} = T_{22}$) were applied in the isotropy plane to preserve the VTI anisotropy ($0 > T_{33} \geq T_{11} > -12$ MPa, minus sign correspond to compressive stresses). Using the set of velocities propagating along and perpendicular to the symmetry axis, as well as off-axis measurements for shale sample, a complete set of second-order VTI elastic constants c^0_{ij} was extracted for each stress state (Prioul et al., 2001). For sandstone, only velocities propagating along the coordinates were available and second-order VTI elastic constants c^0_{ij} were estimated taking the Thomsen parameter $\delta = 0.05$. Then, along-axes quantities (c_{11}, c_{33}, c_{66}, and c_{44}) have been inverted for three third-order constants c_{111}, c_{112}, c_{123} by minimizing the least-squares misfit function (Prioul et al., 2001) between measured stiffnesses and those predicted by equations (1). For the shale sample, this procedure gave the following non-linear constants $c_{111} = -11300 \pm 1000$ GPa, $c_{112} = -4800 \pm 800$ GPa, $c_{123} = 5800 \pm 1300$ GPa for the interval 5 to 20 MPa and $c_{111} = -3100 \pm 200$ GPa, $c_{112} = -800 \pm 150$ GPa, $c_{123} = 40 \pm 250$ GPa for the interval 40 to 100 MPa. Likewise, for the sandstone sample, we obtained $c_{111} = -7400 \pm 800$ GPa, $c_{112} = -1400 \pm 500$ GPa, $c_{123} = 600 \pm 800$ GPa for the whole stress cycle.

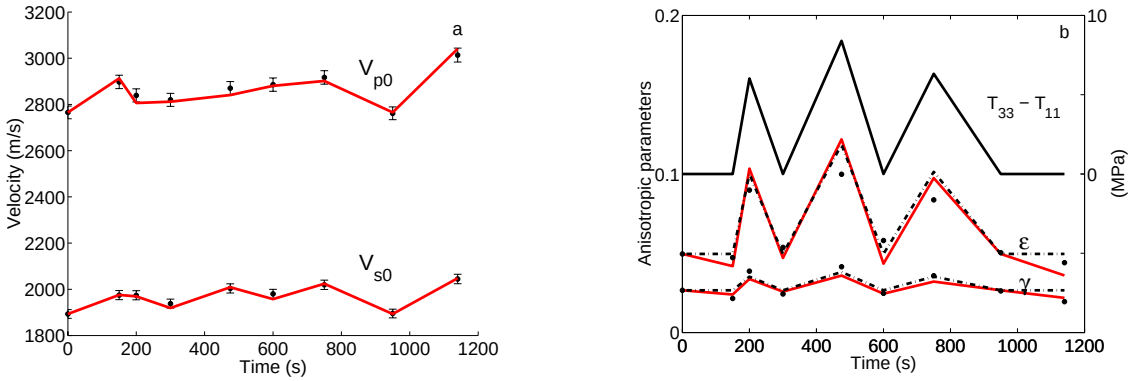

Figure 1: Measured (points) and predicted (lines), (a) V_{P0} and V_{S0}, (b) ε and γ for Colton sandstone under biaxial stress cycle ($T_{33} - T_{11}$). Error bars on measured velocities correspond to $\pm$ 1%.

Thomsen parameters of stressed rocks

The vertical velocities V_{P0} and V_{S0} of P- and S-waves and the three dimensionless Thomsen anisotropic parameters ϵ, δ, and γ can be used as another description of the five elastic coefficients of VTI media. The results displayed on Figures 1 and 2 show that in both set of samples the overall measured V_{P0}, V_{S0} and anisotropic parameters are well described by prediction based on equations (1) and inverted third-order elastic constants, indicating that three "isotropic" third-order coefficients provide a good description in each stress interval.

Here, intuitive insight of the link between stress magnitudes and elastic properties, as well as the link between stress magnitudes and seismic signatures, is allowed using a weak-anisotropy approximation of the Thomsen parameters. Linearizing the equations using these small quantities shows that the Thomsen parameters of stressed rock may be represented as sum of unstressed (or reference state) anisotropies and stress-induced contributions (denoted by subscript s):

$$\epsilon = \epsilon^{(0)} + \epsilon_s, \qquad \delta = \delta^{(0)} + \delta_s, \qquad \gamma = \gamma^{(0)} + \gamma_s \tag{2}$$

$$\epsilon_s = \delta_s = \frac{K_p}{2c_{44}^{(0)}}(T_{11} - T_{33}), \qquad \gamma_s = \frac{K_s}{2c_{44}^{(0)}}(T_{11} - T_{33}) \tag{3}$$

where $K_p = 2c_{155}/c_{33}^{(0)}$ and $K_s = c_{456}/c_{44}^{(0)}$ are the two quantities controlling the stress-induced part of P- and S-wave anisotropy respectively. These quantities are controlled by only two non-linear coefficients c_{155} and $c_{456} = (c_{111} - 3c_{112} + 2c_{123})/8$. As with isotropic media, we note that the stress-induced contributions to VTI rocks also satisfy $\epsilon_s = \delta_s$, which is the condition of elliptical anisotropy.

Colton sandstone. The Colton sandstone was subjected to a biaxial stress and therefore changed its anisotropies throughout the stress cycle (Figure 1). As predicted by the weak-anisotropy equations, the Thomsen parameters start from their unstressed values. For the Colton sample, both the intrinsic and the stress-induced anisotropy were small and therefore weak-anisotropy predictions are almost indistinguishable from exactly computed anisotropic parameters (dash-dotted and solid lines, Figure 1b). Both models provide good quantitative descriptions of experimentally measured anisotropic coefficients, thus confirming the good predictive power of concise weak-anisotropy approximations.

North Sea shale. In the shale experiment, hydrostatic stress was applied, so $T_{11} = T_{22} = T_{33}$. Therefore the weak-anisotropy approximation predicts a constant amount of anisotropy. The results confirm that change in the anisotropic parameters is less than 0.07 for a low confining stress and

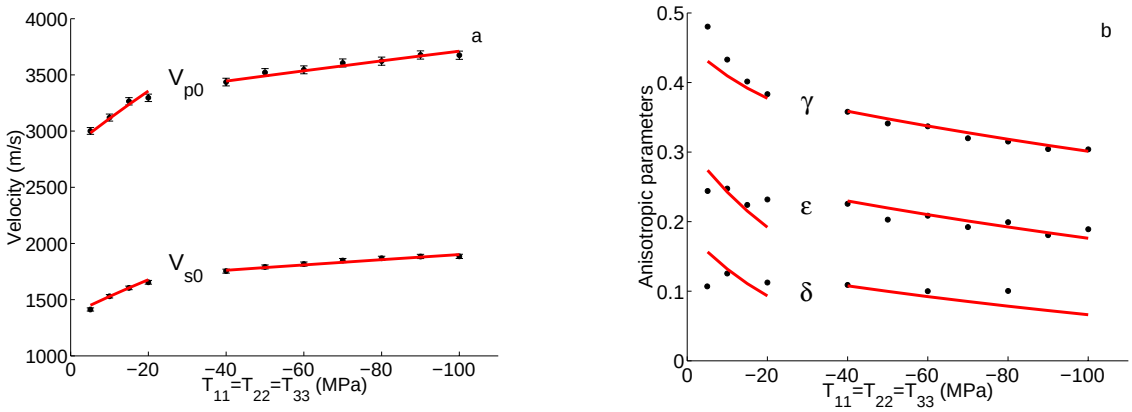

Figure 2: Measured (points) and predicted (lines), (a) V_{P0} and V_{S0}, (b) ε, δ and γ in two intervals of effective confining stress for North Sea shale. Error bars on measured velocities correspond to $\pm$ 1%.

less than 0.05 for a high confining stress, thus being in relatively good agreement with the weak-anisotropy predictions. Higher difference between weak-anisotropy prediction and experiment is due to large intrinsic anisotropy of the shale sample. Exact predictions by non-linear elasticity (solid lines on Figure 2b) are closer to experimental points and predict slight decrease in anisotropic parameters observed with increase in magnitude of confining stress.

Discussion and conclusions

We have proposed a concise and comprehensive way of velocity-stress modelling based on simplified non-linear elasticity theory where both P- and S- ($S1$ and $S2$) wave velocities are treated using the same physical framework. The intrinsic anisotropy of unstressed formations is automatically included and the model allows an arbitrary triaxial stress state ($T_{11} \neq T_{22} \neq T_{33}$) with only three stress-sensitive parameters. As a result *any velocity* in *any direction* can be predicted as a function of stress. In addition, this approach provides simple relationships between Thomsen parameters (controlling seismic signatures) and the differences in magnitudes of principal stresses. Well calibration of the model can be performed directly in situ using multi-mode borehole acoustic measurements (Sinha and Kostek, 1996; Sinha, 2001).

References

Bakulin, V. N. and A. G. Protosenya (1982). Nonlinear effects in travel of elastic waves through rocks. *Proc. USSR Acad. Sc. (Dokl. Akad. Nauk SSSR) 263 (2)*, 214–316.

Dillen, M. W. P., H. M. A. Cruts, J. Groenenboom, J. T. Fokkema, and A. J. W. Duijndam (1999). Ultrasonic velocity and shear-wave splitting behavior of a Colton sandstone under a changing triaxial stress. *Geophysics 64*(5), 1603–1607.

Hornby, B. E. (1995). *The elastic properties of shales.* Cambridge, UK: Ph.D. dissertation, University of Cambridge.

Prioul, R., A. Bakulin, and V. Bakulin (2001). A three-parameter model for predicting acoustic velocities in transversely isotropic rocks under arbitrary stress. In *71st Ann. Internat. Mtg., Soc. Expl. Geophys., Expanded Abstracts*, pp. 1732–1735. Soc. Expl. Geophys.

Sinha, B. K. (2001). Stress-induced changes in the borehole stoneley and flexural dispersions. In *71st Ann. Internat. Mtg., Soc. Expl. Geophys., Expanded Abstracts*, pp. 337–340. Soc. Expl. Geophys.

Sinha, B. K. and S. Kostek (1996). Stress-induced azimuthal anisotropy in borehole flexural waves. *Geophysics 61*, 1899–1907.